JOURNAL OF GUIDANCE, CONTROL, AND DYNAMICS
Vol. 21, No. 1, January–February 1998

Trajectory Tracking for Autonomous Vehicles: An Integrated Approach to Guidance and Control

Isaac Kaminer*
U.S. Naval Postgraduate School, Monterey, California 93943
Antonio Pascoal†
Instituto Superior Técnico, 1096 Lisbon Codex, Portugal
Eric Hallberg‡
U.S. Naval Postgraduate School, Monterey, California 93943
and
Carlos Silvestre§
Instituto Superior Técnico, 1096 Lisbon Codex, Portugal

A new methodology is introduced for integrated design of guidance and control systems for autonomous vehicles (AVs). The methodology proposed borrows from the theory of gain-scheduled control and leads to an efficient procedure for the design of controllers for AVs to accurately track reference trajectories defined in an inertial reference frame. The paper illustrates the application of this procedure to the design of a tracking controller for the unmanned air vehicle Bluebird. The design phase is summarized, and the performance of the resulting controller is assessed in simulation using dynamic models of the vehicle and its sensor suite.

I. Introduction

In a great number of envisioned mission scenarios, autonomous vehicles, including autonomous underwater vehicles (AUVs) and unmanned air vehicles (UAVs), will be required to follow inertial reference trajectories accurately in three-dimensional space. For example, see Refs. 1–3 and the references therein. Similar requirements emerge from the recent work at NASA on descent trajectory synthesis for air traffic control.[4] To achieve this goal, the following systems must be designed and implemented onboard autonomous vehicles (AVs): 1) navigation, to provide estimates of linear and angular positions and velocities of the vehicle, 2) guidance, to process navigation/inertial reference trajectory data and output set points for the vehicle's (body) velocity and attitude, and 3) control, to generate the actuator signals that are required to drive the actual velocity and attitude of the vehicle to the values commanded by the guidance scheme.

The advent of the global positioning system (GPS) has afforded AV systems engineers a powerful new means of obtaining accurate navigation data that is required for precise tracking of given inertial trajectories. However, traditional guidance and control schemes used to steer the vehicle along such trajectories may prove inadequate in the case where frequent heading changes are required or in the presence of shifting wind.[5] Traditionally, such systems are designed separately, using well-established design methods for control and simple strategies such as line of sight (LOS) for guidance. References 6 and 7 contain interesting applications to underwater and air vehicles, respectively. During the design phase, the control system is usually designed with sufficiently large bandwidth to track the commands that are expected from the guidance system. However, because the two systems are effectively coupled, stability and adequate performance of the combined system about nominal trajectories are not guaranteed.[5] In practice, this problem can be resolved by judicious choice of guidance law parameters (such as the visibility distance in LOS strategy), based on extensive computer simulations. Even when stability is obtained, however, the resulting strategy leads to finite trajectory tracking errors, the magnitude of which depends on the type of trajectory to be tracked (radius of curvature, vehicle's desired speed, etc.).[5]

This paper proposes a new methodology for the design of guidance and control systems for AVs whereby the two systems are designed simultaneously. This methodology has two main advantages over traditional ones: 1) the resulting trajectory tracking system achieves zero steady-state tracking error about any trimming trajectory and 2) the design methodology explicitly addresses the problem of stability of the combined guidance and control systems.

Earlier work based on this approach can be found in Refs. 8–10, where the authors introduce a methodology for the design of controllers for AUVs and UAVs to track inertial trajectories that are given in space and time coordinates. The trajectories considered are equilibrium (also known as trimming) trajectories of AVs, which are helices parameterized by the vehicle's linear speed, yaw rate, and flight-path angle. Furthermore, in Refs. 8–10 it is shown the linearization of the vehicle error dynamics and kinematics about any trimming trajectory is time invariant. Thus, the problem of designing integrated guidance and control systems for AVs to accurately track trimming trajectories can be solved by using tools that borrow from gain scheduling control theory, particularly those reported in Ref. 11. Within the framework of Ref. 11, the vehicle's linear speed, yaw rate, and flight-path angle play the role of scheduling variables that interpolate the parameters of linear controllers designed for a finite number of representative trimming trajectories. The results introduced in Ref. 11 on the D implementation of gain scheduled controllers can then be used to obtain a combined guidance/control system such that the properties of the linear designs are recovered locally, about each trimming trajectory. An interesting and very important consequence of the D implementation is that it leads naturally to a controller structure where the only exogenous commands required are the desired linear inertial position and the yaw rate, thus avoiding the need to feedforward the trimming conditions for the remaining state variables and control inputs.

However, the technique presented in Refs. 8–10 has a shortcoming, which may be of concern for UAVs and AUVs, when tracking trimming trajectories in the presence of changing air and water mass. Because the controllers described in those references achieve accurate tracking of trajectories defined in terms of space and time coordinates, the relative speed of the vehicle with respect to the air

Received June 10, 1996; revision received July 20, 1997; accepted for publication July 21, 1997.

*Assistant Professor, Department of Aeronautical and Astronautical Engineering. Member AIAA.
†Associate Professor, Department of Electrical Engineering and Institute for Systems and Robotics (ISR). Member AIAA.
‡Lt. Cdr., U.S. Navy, Department of Aeronautical and Astronautical Engineering.
§Senior Lecturer, Department of Electrical Engineering and Institute for Systems and Robotics (ISR).

or water cannot be controlled externally, its value being computed internally as a function of the tracking error. In practice, this may lead to unacceptable performance in the presence of winds and water currents because the change in the airspeed of the vehicle may result in stall or structural damage.

Clearly, eliminating the time coordinate in the trajectory definition and using the vehicle attitude to null out trajectory errors while maintaining constant airspeed should resolve this problem. A similar approach has been introduced in a number of publications on robot control. Of particular interest is the work reported in Ref. 12, where the subject of path following control for wheeled robots is addressed; also see Ref. 5 for a detailed analysis of the stability of an autonomous underwater vehicle about nominal trajectories in the horizontal plane.

In this paper, these ideas are formalized within the basic framework for three-dimensional trajectory tracking controller system design developed in Refs. 8–10. Using the concepts outlined in Ref. 12, the linear position of an AV is given in terms of its location with respect to the closest point on a desired trajectory, together with the arc length of an imaginary curve traced along that trajectory. Tracking of a trimming trajectory by the vehicle at a fixed speed is then converted into the problem of driving a generalized error vector, which implicitly includes the distance to the trajectory, to zero. Moreover, it is shown that the linearization of the generalized error dynamics about the corresponding trimming path is time invariant. Using these results, the problem of trajectory tracking is posed and solved in the framework of gain scheduled control theory, leading to a new technique for integrated design of guidance and control systems for AVs. The paper summarizes the resulting design methodology and illustrates its application to the design and implementation of a nonlinear trajectory tracking controller for the UAV Bluebird.[10] Numerical simulations using a full set of nonlinear equations of motion of the vehicle show the effectiveness of the proposed techniques.

The subject of trajectory tracking has also been addressed in the literature on control of nonholonomic vehicles. In Ref. 13, the problem of tracking a nominal trajectory by a nonlinear system is considered. The key idea includes linearizing the nonlinear system along the trajectory, then using the resulting time-varying linearization to obtain a time-varying state feedback controller that locally exponentially stabilizes the system along the trajectory. The paper includes examples of applications of the proposed technique to a mobile robot and a front-wheel-drive car. The nominal trajectories considered in Ref. 13 are not restricted to be trimming trajectories. However, all of the examples presented consider the case of trimming trajectories only. Another approach is used in Ref. 14, where a tracking problem for a surface marine vessel is considered. Here the authors use feedback linearization with dynamic extension to obtain a controller to track trajectories that consist of lines and arcs of circles (a special case of trimming trajectories in the plane).

The solution to the trajectory tracking problem proposed in this paper differs considerably from the ones introduced in Refs. 13 and 14. Here, the key idea is to reduce the problem to the design of a tracking controller for a linear time-invariant plant utilizing a simple nonlinear transformation that inverts the vehicle kinematics. This poses no robustness concerns because kinematics are usually well known, particularly in the case of air and underwater vehicles. It is important to point out that the application of the nonlinear transformation results in a nonlinear plant, whose linearization along trimming trajectories is time invariant. Once in the linear setting, the designer is free to choose his favorite control synthesis technique to achieve the desired closed-loop performance and robustness. The paper provides a simple algorithm for implementing the linear controller on the nonlinear plant such that the properties of linear controller are preserved along each trajectory. This is in contrast to the approach in Ref. 13, where the problem is reduced to that of designing an exponentially stabilizing state-feedback controller for a linear time-varying system. This leads to a controller design that is problem specific and does not address the issues of performance and robustness. On the other hand, in Ref. 14 the authors point out that extending to air vehicles the feedback linearization technique use for trajectory tracking of the surface craft is difficult due to the unstable zero dynamics that are characteristic of aircraft.

The paper is organized as follows. Section II develops the rigid-body dynamics and introduces appropriate transformations used in Sec. III to formulate and solve the problem of integrated guidance and control of UAVs. Section IV describes an application to the integrated guidance and control of the UAV Bluebird. Finally, Sec. V contains the main conclusions.

II. Generalized Error Dynamics

We begin this section with a review of the equations of motion of a typical autonomous vehicle such as an airplane or a submarine and introduce the trimming trajectories these vehicles are expected to track. Let $\{I\}$ denote an inertial reference frame, and let $\{B\}$ denote a body coordinate frame that is fixed with respect to the body.

We introduce the following notation suggested by Ref. 15:

P = position of the origin of $\{B\}$ expressed in $\{I\}$
V = linear velocity of the origin of $\{B\}$ relative to $\{I\}$, expressed in $\{B\}$; $(u, v, w)'$
Λ = vector of Euler angles that describe the orientation of frame $\{B\}$ with respect to $\{I\}$; $(\phi, \theta, \psi)'$
Ω = angular velocity of $\{B\}$ relative to $\{I\}$, expressed in $\{B\}$
${}^I_B\mathcal{R}$ = rotation matrix from $\{B\}$ to $\{I\}$; ${}^I_B\mathcal{R}(\Lambda)$
$\mathcal{Q}$ = matrix that relates $(\mathrm{d}/\mathrm{d}t)\Lambda$ to Ω and satisfies the relationships $(\mathrm{d}/\mathrm{d}t)\Lambda = \mathcal{Q}\Omega$ and $\mathcal{Q}(0) = I$; $\mathcal{Q}(\Lambda)$
G = vector of gravitational acceleration expressed in $\{I\}$

We assume a constant gravitational field. Furthermore, let U denote the vector of control inputs acting on the vehicle.

With this notation, the vehicle dynamics can be written in state-space form as follows (see Refs. 16 and 17 for the case of aircraft dynamics and Ref. 9 for the case of underwater vehicle dynamics):

$$\mathcal{G} = \begin{cases} \dfrac{\mathrm{d}}{\mathrm{d}t}V = \mathcal{F}_V(V, \Omega, \Lambda) + \mathcal{I}_V(V, \Omega)\mathcal{H}(V, \Omega, U) \\ \dfrac{\mathrm{d}}{\mathrm{d}t}\Omega = \mathcal{F}_\Omega(V, \Omega, \Lambda) + \mathcal{I}_\Omega(V, \Omega)\mathcal{H}(V, \Omega, U) \\ \dfrac{\mathrm{d}}{\mathrm{d}t}P = {}^I_B\mathcal{R}V \\ \dfrac{\mathrm{d}}{\mathrm{d}t}\Lambda = \mathcal{Q}\Omega \end{cases} \tag{1}$$

where $\mathcal{F}_V$, $\mathcal{F}_\Omega$, $\mathcal{I}_V$, and $\mathcal{I}_\Omega$ are smooth functions.

We are interested in the development of guidance and control systems to steer an autonomous vehicle along prescribed inertial trajectories $P_C(t) \in \Re^3$. Furthermore, we require that the vehicle be trimmed along any such trajectory. This requirement is reasonable because most of the applications for autonomous vehicles today call for trimmed flight. Let $\{C\}$ define a coordinate system attached to the vehicle and let Λ_C define the desired inertial orientation of $\{C\}$. The coordinate system $\{C\}$ represents the desired inertial orientation of the vehicle along P_C. Therefore, at trim $\{C\} = \{B\}$. Next we define the set $\mathcal{E}$ of the trimming trajectories about which the vehicle is expected to operate:

$$\mathcal{E} := \left\{ \begin{bmatrix} P_C \\ \Lambda_C \end{bmatrix} : \begin{array}{l} \dfrac{\mathrm{d}}{\mathrm{d}t}P_C = {}^I_C\mathcal{R}V_C \\ \dfrac{\mathrm{d}}{\mathrm{d}t}\Lambda_C = \mathcal{Q}(\Lambda_C)\Omega_C =: \mathcal{Q}_C\Omega_C \\ \mathcal{F}_V(V_C, \Omega_C, \Lambda_C) \\ \quad + \mathcal{I}_V(V_C, \Omega_C)\mathcal{H}(V_C, \Omega_C, U_c) = 0 \\ \mathcal{F}_\Omega(V_C, \Omega_C, \Lambda_C) \\ \quad + \mathcal{I}_\Omega(V_C, \Omega_C)\mathcal{H}(V_C, \Omega_C, U_c) = 0 \end{array} \right\} \tag{2}$$

where V_C, Ω_C, and U_c denote the trimming values of V, Ω, and U, respectively, and Λ_C denotes the vector of Euler angles that describe the orientation of $\{C\}$ with respect to $\{I\}$.

From the definition of $\mathcal{E}$ and Eqs. (1) it can be concluded[16] that the only possible trimming trajectories $P_C \in \mathcal{E}$ correspond to helices

$$\frac{\mathrm{d}}{\mathrm{d}t}\Lambda_C = \begin{bmatrix} 0 \\ 0 \\ \dot{\psi}_C \end{bmatrix}, \qquad \frac{\mathrm{d}}{\mathrm{d}t}P_C = \begin{bmatrix} -v_c \cos(\gamma_C)\sin(\dot{\psi}_C t) \\ v_c \cos(\gamma_C)\cos(\dot{\psi}_C t) \\ -v_c \sin(\gamma_C) \end{bmatrix} \tag{3}$$

where $\dot{\psi}_C$, $v_c = \|V_C\|$, and γ_C denote desired yaw rate, inertial velocity, and flight-path angle, respectively, of the vehicle along P_C. Thus, the trimming trajectories can be parameterized by the vector

$$\eta_c = [v_c, \dot{\psi}_C, \gamma_C]' \in \Re^3 \tag{4}$$

In fact, given η_c we can determine the trimming values for V_C, Ω_C, and U_C. A detailed derivation of trimming trajectories for the case of an unmanned air vehicle is given in Sec. IV.

Integrating Eq. (3) we obtain

$$P_C(t) = \begin{bmatrix} \dfrac{v_c \cos(\gamma_C)}{\dot{\psi}_C}\cos(\dot{\psi}_C t) \\ \dfrac{v_c \cos(\gamma_C)}{\dot{\psi}_C}\sin(\dot{\psi}_C t) \\ -v_c \sin(\gamma_C) t \end{bmatrix} \tag{5}$$

Equation (5) indicates that the radius of the helix is $r := v_c \cos(\gamma_C)/\dot{\psi}_C$ and the climb rate is $\dot{h}_c := -v_c \sin(\gamma_C)$. Using elementary ideas from differential geometry[18] Eq. (5) can be reparametrized by utilizing the arclength

$$s := \int \left\| \frac{\mathrm{d}}{\mathrm{d}t}P_C(t) \right\| \mathrm{d}t = \int v_c \, \mathrm{d}t$$

to obtain

$$P_C(s) = \begin{bmatrix} r\cos[\dot{\psi}_C(s/v_c)] \\ r\sin[\dot{\psi}_C(s/v_c)] \\ -h_C(s/v_c) \end{bmatrix} \tag{6}$$

Now, let $\{A\}$ denote a Frenet frame attached to $P_C(s)$ (Ref. 18). Then the x, y, and z axis of $\{A\}$ can be defined using the orthonormal vectors T, N, and B, where $T(s)$ is a unit vector tangent to $P_C(s)$ at s,

$$T(s) = \frac{\mathrm{d}P(s)}{\mathrm{d}s} = \begin{bmatrix} -(r\dot{\psi}_C/v_c)\sin[\dot{\psi}_C(s/v_c)] \\ (r\dot{\psi}_C/v_c)\cos[\dot{\psi}_C(s/v_c)] \\ -\dot{h}/v_c \end{bmatrix}$$

$$= \begin{bmatrix} -\cos(\gamma_C)\sin[\dot{\psi}_C(s/v_c)] \\ \cos(\gamma_C)\cos[\dot{\psi}_C(s/v_c)] \\ -\sin(\gamma_C) \end{bmatrix}$$

Similarly, $N(s) = [\mathrm{d}T(s)/\mathrm{d}s]/\kappa(s)$, where $\kappa(s) := \|\mathrm{d}T(s)/\mathrm{d}s\|$ is called the curvature of $P_C(s)$. Then,

$$N(s) = \begin{bmatrix} -\cos[\dot{\psi}_C(s/v_c)] \\ -\sin[\dot{\psi}_C(s/v_c)] \\ 0 \end{bmatrix}$$

and $\kappa(s) = \dot{\psi}_C \cos(\gamma_c)/v_c$. It follows that $B(s) = T(s) \times N(s)$,

$$B(s) = \begin{bmatrix} \sin(\gamma_C)\sin[\dot{\psi}_C(s/v_c)] \\ -\sin(\gamma_C)\cos[\dot{\psi}_C(s/v_c)] \\ \cos(\gamma_C) \end{bmatrix}$$

Finally, the coordinate transformation ${}^I_A\mathcal{R}$ from $\{A\}$ to $\{I\}$ is given by ${}^I_A\mathcal{R} = [T \quad N \quad B]$. Furthermore, using the Serret–Frenet Theorem[18] we obtain

$$\frac{\mathrm{d}}{\mathrm{d}t}{}^I_A\mathcal{R} = \frac{\mathrm{d}{}^I_A\mathcal{R}}{\mathrm{d}s}\dot{s} = [T \quad N \quad B]\begin{bmatrix} 0 & -\kappa & 0 \\ \kappa & 0 & -\tau \\ 0 & \tau & 0 \end{bmatrix}\dot{s} = {}^I_A\mathcal{R}\mathcal{S}({}^A\Omega)$$

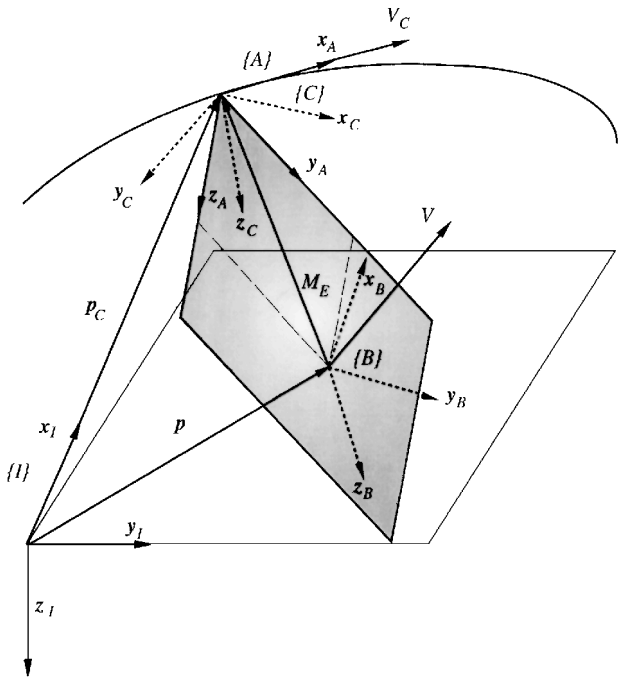

Fig. 1 Trajectory tracking: basic three-dimensional geometry.

where $\tau(s)$ is the torsion of $P(s)$, given by $\tau(s) = \dot{h}\dot{\psi}_C/v_c^2 = \dot{\psi}_C \sin\gamma_c/v_c$; ${}^A\Omega = [\tau\dot{s} \;\; 0 \;\; \kappa\dot{s}]^T$ is the angular velocity of $\{A\}$ with respect to $\{I\}$, resolved in $\{A\}$; and $\mathcal{S}(Y)$ is a skew symmetric matrix defined by $\mathcal{S}(Y) = Y\times$ (Ref. 15), where $\times$ denotes cross product.

Let $P_C(s_0)$ denote the point on the trajectory $P_C \in \mathcal{E}$ the shortest distance away from the vehicle's position P (see Fig. 1). We call $P_C(s_0)$ a projection of P onto $P_C \in \mathcal{E}$. (For the discussion of when such a point can be uniquely determined, see Ref. 12.) Define the error vector $M_E := {}^A_I\mathcal{R}(P - P_C(s_0))$. Then M_E will necessarily have the following form (see Fig. 1):

$$M_E = [0 \quad y \quad z]$$

Using definitions of M_E and $\{A\}$, we obtain

$$\frac{\mathrm{d}}{\mathrm{d}t}P = \frac{\mathrm{d}}{\mathrm{d}t}P_C + \frac{\mathrm{d}}{\mathrm{d}t}\left({}^I_A\mathcal{R}M_E\right)$$

$$\Rightarrow {}^I_B\mathcal{R}V = {}^I_A\mathcal{R}\begin{bmatrix} \dot{s} \\ 0 \\ 0 \end{bmatrix} + {}^I_A\mathcal{R}\mathcal{S}({}^A\Omega)M_E + {}^I_A\mathcal{R}\begin{bmatrix} 0 \\ \dot{y} \\ \dot{z} \end{bmatrix}$$

$$\Rightarrow \begin{bmatrix} \dot{s} \\ \dot{y} \\ \dot{z} \end{bmatrix} + \mathcal{S}({}^A\Omega)M_E = {}^A_I\mathcal{R}{}^I_B\mathcal{R}V = {}^A_B\mathcal{R}V$$

Simple algebra shows that

$$\begin{bmatrix} \dot{s} \\ \dot{y} \\ \dot{z} \end{bmatrix} = \begin{bmatrix} 1 - y\kappa & 0 & 0 \\ z\tau & 1 & 0 \\ y\tau & 0 & 1 \end{bmatrix}^{-1} {}^A_B\mathcal{R}V \tag{7}$$

The design of an integrated guidance and control system for the plant $\mathcal{G}$ in Eq. (1) and the set $\mathcal{E}$ involves obtaining linear models for $\mathcal{G}$ along the trajectories in $\mathcal{E}$. These models will necessarily be time varying in the state-space coordinates used in Eq. (1). It turns out, however, that an appropriate coordinate system exists where the linearization of the plant $\mathcal{G}$ along any trajectory $P_C \in \mathcal{E}$ is time invariant. This coordinate system is discussed next. Let P_C, $\Lambda_C \in \mathcal{E}$ be given. Define

$$\begin{aligned} V_E &= V - V_C, & \Omega_E &= \Omega - \Omega_C \\ P_E &= [s \quad y \quad z]', & \Lambda_E &= \mathcal{Q}^{-1}(\Lambda - \Lambda_C) \end{aligned} \tag{8}$$

which can be interpreted as the generalized error vector between the vehicle state and the trajectory in $\mathcal{E}$. Simple physical considerations

show that the problem of following a trimming trajectory $P_C \in \mathcal{E}$ at a fixed speed V_C is equivalent to driving the generalized error vector to zero.

Next, by noticing that V_C and Ω_C are constant along trimming trajectories, we obtain the generalized error dynamics (see the Appendix):

$$\mathcal{G}_E = \begin{cases} \dfrac{\mathrm{d}}{\mathrm{d}t} V_E = \mathcal{F}_{V_E}(V_E, \Omega_E, \Lambda_E) \\ \quad + \mathcal{I}_{V_E}(V_E, \Omega_E)\mathcal{H}(V_E, \Omega_E, U) \\ \dfrac{\mathrm{d}}{\mathrm{d}t}\Omega_E = \mathcal{F}_{\Omega_E}(V_E, \Omega_E, \Lambda_E) \\ \quad + \mathcal{I}_{\Omega_E}(V_E, \Omega_E)\mathcal{H}(V_E, \Omega_E, U) \\ \dfrac{\mathrm{d}}{\mathrm{d}t} P_E = \begin{bmatrix} 1 - y\kappa & 0 & 0 \\ z\tau & 1 & 0 \\ y\tau & 0 & 1 \end{bmatrix}^{-1} {}_B^A\mathcal{R} V \\ \dfrac{\mathrm{d}}{\mathrm{d}t}\Lambda_E = \Omega_E - \Omega_C - \mathcal{Q}^{-1}\mathcal{Q}_C\Omega_C + \dot{\mathcal{Q}}^{-1}\mathcal{Q}\Lambda_E \end{cases} \tag{9}$$

where

$$\mathcal{F}_{V_E}(V_E, \Omega_E, \Lambda_E) = \mathcal{F}_V(V_E + V_C, \Omega_E + \Omega_C, \mathcal{Q}\Lambda_E + \Lambda_C)$$

and similarly for $\mathcal{I}_{V_E}$, $\mathcal{F}_{\Omega_E}$, and $\mathcal{I}_{\Omega_E}$. It can be shown that the linearization of Eqs. (9) along any trajectory $P_C \in \mathcal{E}$ is time invariant and is given by (see the Appendix)

$$\mathcal{G}_l(\eta_c) = \begin{cases} \dfrac{\mathrm{d}}{\mathrm{d}t}\delta V_E = \mathcal{A}_V^V \delta V_E + \mathcal{A}_V^\Omega \delta\Omega_E + \mathcal{A}_V^\Lambda \delta\Lambda_E + \mathcal{B}_V \delta U \\ \dfrac{\mathrm{d}}{\mathrm{d}t}\delta\Omega_E = \mathcal{A}_\Omega^V \delta V_E + \mathcal{A}_\Omega^\Omega \delta\Omega_E + \mathcal{A}_\Omega^\Lambda \delta\Lambda_E + \mathcal{B}_\Omega \delta U \\ \dfrac{\mathrm{d}}{\mathrm{d}t}\delta P_E = \left({}_C^A\mathcal{R} V_C\right)_x \begin{bmatrix} 0 & \kappa & 0 \\ 0 & 0 & -\tau \\ 0 & -\tau & 0 \end{bmatrix} \delta P_E \\ \quad - {}_C^A\mathcal{R}\mathcal{S}(V_C)\delta\Lambda_E + {}_C^A\mathcal{R}\delta V_E \\ \dfrac{\mathrm{d}}{\mathrm{d}t}\delta\Lambda_E = \delta\Omega_E - \mathcal{S}(\Omega_C)\delta\Lambda_E \end{cases} \tag{10}$$

where

$$\mathcal{A}_X^Y \equiv \frac{\partial}{\partial Y}[\mathcal{F}_X(\cdot) + \mathcal{I}_X(\cdot)\mathcal{H}(\cdot)], \qquad \mathcal{B}_Z \equiv \frac{\partial}{\partial Z}[\mathcal{I}_X(\cdot)\mathcal{H}(\cdot)]$$

are computed at the equilibrium values of V, Ω, and U, and $({}_C^A\mathcal{R} V_C)_x$ is the x component of the vector ${}_C^A\mathcal{R} V_C$. In the sequel we will use the symbol $\mathcal{G}_l$ to denote the set of all linear plants $\mathcal{G}_l(\eta_c)$ associated with the set $\mathcal{E}$.

III. Trajectory Tracking Control System Design and Implementation

In the preceding section we have shown that the linearization of the nonlinear system $\mathcal{G}_E$ about any trajectory in $\mathcal{E}$ results in a time-invariant plant $\mathcal{G}_l(\eta_c)$. Therefore, associated with the set $\mathcal{E}$ there is a family of linear plants $\mathcal{G}_l$, which can now be used to synthesize a tracking (possibly gain scheduled) controller $\mathcal{C}$ designed to operate over all of the trajectories in $\mathcal{E}$.

A common approach to the development of such a controller $\mathcal{C}$ requires designing a family of linear controllers for a finite number of linear plants in $\mathcal{G}_l$ and then interpolating between these controllers to achieve adequate performance for all of the linearized plants in $\mathcal{G}_l$. During real time operation, the controller parameters are updated as functions of a gain scheduling variable $q = h(V, \Omega, \Lambda, P, U, \eta_c)$, where h is a C^1 function. For example, a typical gain scheduling variable for the case of aircraft is dynamic pressure $q = \frac{1}{2}\rho\|V\|^2$, where ρ represents air density.

In what follows, we restrict ourselves to the idealized case where the description of each controller for each plant $\mathcal{G}_l(\eta_c)$ is available.[19] Therefore, we assume that the first design step produces the set

$$\mathcal{C}_l := \{\mathcal{C}_l(q_c), \quad q_c = h(V_C, \Omega_C, \Lambda_C, P_C, U_c, \eta_c)\}$$

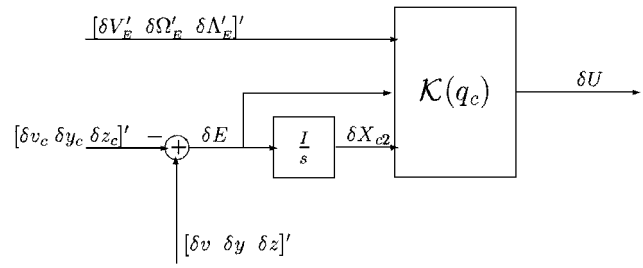

$$\mathcal{K}(q_c) = \left[\begin{array}{c|ccc} A_{c1}(q_c) & B_{c1}(q_c) & B_{c2}(q_c) & B_{c3}(q_c) \\ \hline C_{c1}(q_c) & D_{c1}(q_c) & D_{c2}(q_c) & D_{c3}(q_c) \end{array}\right]$$

Fig. 2 Linear controller $\mathcal{C}_l(q_c)$.

given by (see Fig. 2)

$$\mathcal{C}_l(q_c) = \begin{cases} \delta E = [\delta v \quad \delta y \quad \delta z]' - [\delta v_c \quad \delta y_c \quad \delta z_c]' \\ \dfrac{\mathrm{d}}{\mathrm{d}t}\delta X_{c1} = \mathcal{A}_{c1}(q_c)\delta X_{c1} + \mathcal{B}_{c1}(q_c)[\delta V_E' \ \delta\Omega_E' \ \delta\Lambda_E']' \\ \quad + \mathcal{B}_{c2}(q_c)\delta X_{c2} + \mathcal{B}_{c3}(q_c)\delta E \\ \dfrac{\mathrm{d}}{\mathrm{d}t}\delta X_{c2} = \delta E \\ \delta U = \mathcal{C}_{c1}(q_c)\delta X_{c1} + \mathcal{D}_{c1}(q_c)[\delta V_E' \quad \delta\Omega_E' \quad \delta\Lambda_E']' \\ \quad + \mathcal{D}_{c2}(q_c)\delta X_{c2} + \mathcal{D}_{c3}(q_c)\delta E \end{cases} \tag{11}$$

where the vector δX_{c2} represents the integrator states of the controller $\mathcal{C}_l(q_c)$, the vector δX_{c1} represents the remaining states of the controller $\mathcal{C}_l(q_c)$, $\delta X_{c1} \in R^{n_c}$, $\delta X_{c2} \in R^m$, $m = \dim(U)$,

$$[\delta v \quad \delta y \quad \delta z]' = \mathcal{C}_1[\delta V_E' \quad \delta\Omega_E' \quad \delta\Lambda_E']' + \mathcal{C}_2\delta P_E$$

$\mathcal{C}_1 = [V_C'/\|V_C\| \ \ 0 \ \ 0], \mathcal{C}_2 = \mathrm{diag}[0 \ \ 1 \ \ 1]$, and the commands δy_c and δz_c are introduced to determine how fast the error states δy and δz go to zero. We further assume that the parameters of the controller are C^1 functions of q_c.

The structure of the controller $\mathcal{C}_l(q_c)$ has the following important feature. Suppose the closed-loop system consisting of $\mathcal{G}_l(q_c)$ and $\mathcal{C}_l(q_c)$ given by Eqs. (10) and (11) is asymptotically stable. Then for given q_c the controller $\mathcal{C}_l(q_c)$ will ensure zero steady-state error to a step input for the variables in δE. This includes errors in the vehicle's inertial velocity v and in the deviations from P_C, z, and y. Zero steady-state errors are achieved by integrating δE. This structure is typical of tracking controllers, because they are designed to drive errors between step changes in reference commands and the corresponding plant outputs to zero in steady state. Notice that the block $\mathcal{K}(q_c)$ (see Fig. 2) may itself contain additional integrators.

Next, the family of linear controllers $\mathcal{C}_l(q_c)$ must be implemented on the nonlinear plant $\mathcal{G}$ defined in Sec. II. This problem has been addressed in Ref. 11 for the general class of nonlinear plants and for tracking controllers with the same structure as $\mathcal{C}_l(q_c)$. In Ref. 11 the authors formulated a so-called controller implementation problem, which will be repeated here for the problem at hand.

Let $\mathcal{T}(\mathcal{G}(q_c), \mathcal{C}_l(q_c))$ be the closed-loop linear system that results from connecting $\mathcal{C}_l(q_c)$ to $\mathcal{G}_l(q_c)$, and denote by $T(\mathcal{G}_l(q_c), \mathcal{C}_l(q_c))$ the corresponding matrix transfer function. Let $\mathcal{T}(\mathcal{G}, \mathcal{C})(q_c)$ be the nonlinear closed-loop system that consists of $\mathcal{C}$ and $\mathcal{G}$, and let $\mathcal{T}_l(\mathcal{G}, \mathcal{C})(q_c)$ denote its linearization about $P_C \in \mathcal{E}$ and denote by $T_l(\mathcal{G}, \mathcal{C})(q_c)$ the corresponding matrix transfer function. With this notation, the controller implementation problem applied to the integrated guidance and control problem considered in this paper can be stated as follows: Find a gain scheduled controller $\mathcal{C}$ such that for each trajectory $P_C \in \mathcal{E}$ 1) the feedback systems $\mathcal{T}_l(\mathcal{G}, \mathcal{C})(q_c)$ and $\mathcal{T}(\mathcal{G}_l(q_c), \mathcal{C}_l(q_c))$ have the same closed-loop eigenvalues and 2) the closed-loop transfer functions $T_l(\mathcal{G}, \mathcal{C})(q_c)$ and $T(\mathcal{G}_l(q_c), \mathcal{C}_l(q_c))$ are equal.

In the sequel we provide a complete solution to the controller implementation problem. Given the set $\mathcal{C}_l$ of linear controllers for

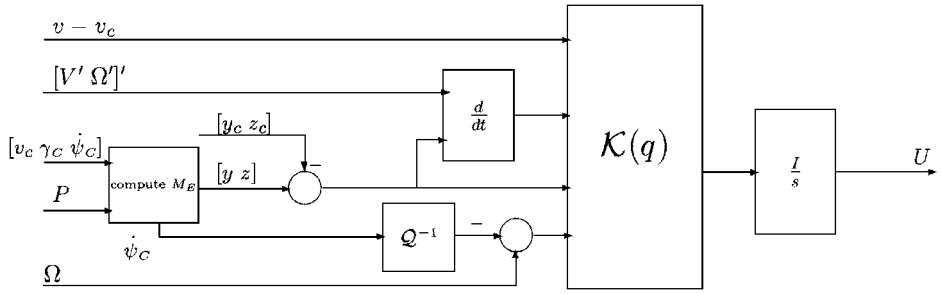

Fig. 3 Nonlinear controller C.

the set $\mathcal{G}_l$ of linearized plant models, we propose the following structure for the gain scheduled controller $\mathcal{C}$ (see Fig. 3):

$$\mathcal{C} := \begin{cases} [0 \quad y \quad z]' = {}^{A}_{I}\mathcal{R}(P - P_C(s_0)) \\ E = [v - v_c \quad y - y_c \quad z - z_c] \\ \dfrac{\mathrm{d}}{\mathrm{d}t}X_{c1} = \mathcal{A}_{c1}(q)X_{c1} + \mathcal{B}_{c1}(q)\left[\dfrac{\mathrm{d}}{\mathrm{d}t}V' \quad \dfrac{\mathrm{d}}{\mathrm{d}t}\Omega' \quad \left(\Omega - \mathcal{Q}^{-1}\dot{\Lambda}_C\right)'\right]' + \mathcal{B}_{c2}(q)E + \mathcal{B}_{c3}(q)\dfrac{\mathrm{d}}{\mathrm{d}t}E \\ \dfrac{\mathrm{d}}{\mathrm{d}t}X_{c2} = \mathcal{C}_{c1}(q)X_{c1} + \mathcal{D}_{c1}(q)\left[\dfrac{\mathrm{d}}{\mathrm{d}t}V' \quad \dfrac{\mathrm{d}}{\mathrm{d}t}\Omega' \quad (\Omega - \mathcal{Q}^{-1}\dot{\Lambda}_C)'\right]' + \mathcal{D}_{c2}(q)E + \mathcal{D}_{c3}(q)\dfrac{\mathrm{d}}{\mathrm{d}t}E \\ U = X_{c2} \end{cases} \tag{12}$$

where $P_C(s_0)$ is the projection of P onto the helix $P_C \in \mathcal{E}$. The algorithm for computing $P_C(s_0)$ and s_0 is given in the Appendix. Comparison of Figs. 2 and 3 indicates that the structure of the gain scheduled controller is easily obtained from that of the linear controllers. We now make the following assumptions.

Assumption 1: $\mathrm{Dim}(X_{c2}) = \dim(U) = \dim(E)$.

Assumption 2: The matrix

$$\begin{bmatrix} sI - \mathcal{A}_{c1}(q) & \mathcal{B}_{c3}(q) \\ -\mathcal{C}_{c1}(q) & \mathcal{D}_{c3}(q) \end{bmatrix}$$

has full rank at $s = 0$ for each $P_C \in \mathcal{E}$.

Assumption 3: The matrix pair $(\mathcal{A}_{c1}, \mathcal{C}_{c1})$ is observable.

Assumption 1 implies that the number of integrators is equal to the number of control inputs. This is necessary if the controller is to provide independent control of the errors E using the control inputs U. Assumption 2 implies that the realization $(\mathcal{A}_{c1}, \mathcal{B}_{c2}, \mathcal{C}_{c1}, \mathcal{D}_{c2})$ has no transmission zeros at the origin. Finally, Assumption 3 guarantees that the state X_{c1} is zero along the trajectories in $\mathcal{E}$.

The main result of this section is stated next.

Theorem 1: Suppose Assumptions 1 and 2 hold. Then the gain scheduled controller $\mathcal{C}$ given by Eqs. (12) solves the controller implementation problem, i.e., for each $P_C \in \mathcal{E}$ the following properties hold:

1) The feedback systems $\mathcal{T}_l(\mathcal{G}, \mathcal{C})(q_c)$ and $\mathcal{T}(\mathcal{G}_l(q_c),\ \mathcal{C}_l(q_c))$ have the same closed-loop eigenvalues.

2) The closed-loop matrix transfer functions $T_l(\mathcal{G}, \mathcal{C})(q_c)(s)$ and $T(\mathcal{G}_l(q_c), \mathcal{C}_l(q_c))(s)$ are equal.

Thus, the eigenvalues of the linearizations along each trajectory in $\mathcal{E}$ are preserved; furthermore, the input–output behavior of the linearized operators is preserved in a well-defined sense. The reader is referred to Ref. 11 for a complete discussion on approximations to this method that avoid using pure differentiation.

Theorem 1 can be used as follows: First, determine the dynamics of the autonomous vehicle $\mathcal{G}$ and the set of trimming trajectories $\mathcal{E}$ the vehicle is required to track. This set is parametrized by the range of trimming velocities v_c, desired flight-path angles γ_c, and desired heading rates $\dot{\psi}_c$. Recall, these variables constitute a gain scheduling vector $q_c = [v_c \ \ \gamma_c \ \ \dot{\psi}_c]'$. Next, rewrite the vehicle dynamics using generalized error coordinates V_E, Ω_E, Λ_E, and P_E to obtain the vehicle's error dynamics $\mathcal{G}_E$. Linearize $\mathcal{G}_E$ about a finite number of trajectories in $\mathcal{E}$. Use these linear models to design a finite number (k) of trajectory tracking controllers $\{\mathcal{C}_{l_i}, i = 1, k\}$. Gain schedule $\{\mathcal{C}_{l_i}, i = 1, k\}$ utilizing a favorite interpolation or gain scheduling technique to obtain the linear gain scheduled controller $\mathcal{C}_l(q_c)$. Now implement this controller on the nonlinear plant $\mathcal{G}$ according to the expression (12).

Proof: In the proof we set the controller matrices $\mathcal{D}_{c1}$ and $\mathcal{D}_{c3}$ to zero. This does not change the results but simplifies considerably the algebra. Furthermore, we will drop explicit dependence of the controller parameters on the gain scheduling variable q.

Let $P_C \in \mathcal{E}$ be given. Consider the feedback interconnection of the linear plant $\mathcal{G}_l(q_c)$ and linear controller $\mathcal{C}_l(q_c)$. The state matrix F of this feedback system has the following form:

$$F := \begin{bmatrix} \mathcal{A}_1 & 0 & \mathcal{B}\mathcal{C}_{c1} & \mathcal{B}\mathcal{D}_{c2} \\ \mathcal{A}_2 & \mathcal{A}_3 & 0 & 0 \\ \mathcal{B}_{c1} + \mathcal{B}_{c3}\mathcal{C}_1 & \mathcal{B}_{c3}\mathcal{C}_2 & \mathcal{A}_{c1} & \mathcal{B}_{c2} \\ C_1 & C_2 & 0 & 0 \end{bmatrix} \tag{13}$$

where

$$\mathcal{A}_1 = \begin{bmatrix} \mathcal{A}_V^V & \mathcal{A}_V^\Omega & \mathcal{A}_V^\Lambda \\ \mathcal{A}_\Omega^V & \mathcal{A}_\Omega^\Omega & \mathcal{A}_\Omega^\Lambda \\ 0 & I & -\mathcal{S}(\Omega_C) \end{bmatrix}$$

$$\mathcal{A}_2 = \begin{bmatrix} {}^{A}_{C}\mathcal{R} & 0 & -{}^{A}_{C}\mathcal{R}\mathcal{S}(V_C) \end{bmatrix}$$

$$\mathcal{A}_3 = \left({}^{A}_{C}\mathcal{R}V_C\right)_x \begin{bmatrix} 0 & \kappa & 0 \\ 0 & 0 & -\tau \\ 0 & -\tau & 0 \end{bmatrix}$$

$$\mathcal{B} = [\mathcal{B}_V' \quad \mathcal{B}_\Omega' \quad 0]', \qquad \left({}^{A}_{C}\mathcal{R}V_C\right)_x = x \text{ component of } {}^{A}_{C}\mathcal{R}V_C$$

Next we linearize the feedback interconnection of the plant $\mathcal{G}$ and the controller $\mathcal{C}$. However, to do that, first we must determine the values of the controller states X_{c1} and X_{c2} along the trajectory $P_C \in \mathcal{E}$. From Eq. (12) we obtain

$$\frac{\mathrm{d}}{\mathrm{d}t}X_{c1_c} = \mathcal{A}_{c1}X_{c1_c} + \mathcal{B}_{c1}\left[\frac{\mathrm{d}}{\mathrm{d}t}V_C' \quad \frac{\mathrm{d}}{\mathrm{d}t}\Omega_C' \quad \left(\Omega_C - \mathcal{Q}_C^{-1}\dot{\Lambda}_C\right)'\right]'$$

$$+ \mathcal{B}_{c2}E_C + \mathcal{B}_{c3}\frac{\mathrm{d}}{\mathrm{d}t}E_C$$

$$\frac{\mathrm{d}}{\mathrm{d}t}X_{c2_c} = \mathcal{C}_{c1}X_{c1_c} + \mathcal{D}_{c2}E_C, \qquad U_c = X_{c2_c}$$

Notice, because along $P_C \in \mathcal{E}$,

$$E_C = 0, \qquad V_C = \text{const}, \qquad \Omega_C = \text{const}$$
$$\Omega_C - \mathcal{Q}_C^{-1}\dot{\Lambda}_C = 0, \qquad X_{c2_c} = U_c = \text{const}$$

we get

$$\frac{\mathrm{d}}{\mathrm{d}t}X_{c1_c} = \mathcal{A}_{c1}X_{c1_c}, \qquad 0 = \mathcal{C}_{c1}X_{c1_c}$$

Now, using Assumption 3 we conclude that $X_{c1_c} = 0$.

To compute the linearization of the feedback interconnection of $\mathcal{G}$ and $\mathcal{C}$ ($\mathcal{T}(\mathcal{G},\mathcal{C})$) along $P_C \in \mathcal{E}$, observe that $\mathcal{F}(\mathcal{G},\mathcal{C})$ is equal to the feedback interconnection of $\mathcal{G}_E$ and the system consisting of $\mathcal{K}(q)$ and the integrator X_{c2}. The linearization of $\mathcal{G}_E$ along $P_C \in \mathcal{E}$ is given by Eqs. (10). The linearization of the system consisting of $\mathcal{K}(q)$ and X_{c2} can be obtained using the trimming values of X_{c1} and X_{c2} and the steps outlined in the proof of Theorem 4.1 in Ref. 11. For brevity of exposition the detailed derivation is omitted. The linearization has the following form:

$$\begin{aligned}\frac{\mathrm{d}}{\mathrm{d}t}\delta X_{c1} &= \mathcal{A}_{c1}\delta X_{c1} + \mathcal{B}_{c1}\left[\frac{\mathrm{d}}{\mathrm{d}t}\delta V_C' \quad \frac{\mathrm{d}}{\mathrm{d}t}\delta\Omega'_C \quad \frac{\mathrm{d}}{\mathrm{d}t}\delta\Lambda'_E\right]' \\ &\quad + \mathcal{B}_{c2}\delta E + \mathcal{B}_{c3}\frac{\mathrm{d}}{\mathrm{d}t}\delta E \qquad (14)\\ \frac{\mathrm{d}}{\mathrm{d}t}\delta X_{c2} &= \mathcal{C}_{c1}\delta X_{c1} + \mathcal{D}_{c2}\delta E, \qquad \delta U = \delta X_{c2}\end{aligned}$$

It is easy to verify that the state matrix M of $\mathcal{T}_l(\mathcal{G},\mathcal{C})$ is

$$M = \left[\begin{array}{cc|c|c} \mathcal{A}_1 & 0 & 0 & \mathcal{B} \\ \mathcal{A}_2 & \mathcal{A}_3 & 0 & 0 \\ \hline [\mathcal{B}_{c1} \;\; \mathcal{B}_{c3}]\begin{bmatrix} I & 0 \\ \mathcal{C}_1 & \mathcal{C}_2 \end{bmatrix}\begin{bmatrix} \mathcal{A}_1 & 0 \\ \mathcal{A}_2 & \mathcal{A}_3 \end{bmatrix} + \mathcal{B}_{c2}[\mathcal{C}_1 \;\; \mathcal{C}_2] & \mathcal{A}_{c1} & [\mathcal{B}_{c1} \;\; \mathcal{B}_{c3}]\begin{bmatrix} I & 0 \\ \mathcal{C}_1 & \mathcal{C}_2 \end{bmatrix}\begin{bmatrix} B \\ 0 \end{bmatrix} \\ \hline D_{c2}[C_1 \;\; C_2] & \mathcal{C}_{c1} & 0 \end{array}\right]$$

The proof of the first part of the theorem now follows from Assumption 2 and an observation that the matrices F and M are in the form of the matrices F and M in the proof of the Theorem 4.1 in Ref. 11.

The proof of the second part of the theorem follows directly from the proof of the second part of Theorem 4.1 in Ref. 11. □

It is worth emphasizing the following important properties of the controller $\mathcal{C}$. 1) The result in Theorem 1 holds for all trajectories in $\mathcal{E}$. 2) The structure of the controller $\mathcal{C}$ is easily obtained from that of the linear controllers. 3) Because all of the closed-loop transfer functions of the local linearizations are preserved, at the level of local linear analysis, the controller does not introduce any additional noise amplification despite the presence of a differentiation operator. 4) Along trajectories $P_C \in \mathcal{E}$, $X_{c2_c} = U_c$ and $X_{c1_c} = 0$. Therefore, the trimming values of the control inputs are naturally provided by the integrator block with state X_{c2_c}. 5) The integrators X_{c2} are directly at the input of the plant, which makes it straightforward to implement antiwindup schemes. This becomes necessary in applications where the input U is hard limited due to actuator saturation, for example. 6) The inputs to the controller P_C and $\dot{\Lambda}_C$ can be computed directly from the vector q_c. 7) The trim values V_C, Ω_C, and U_c are not required in the controller implementation. 8) Along the trajectories $P_C \in \mathcal{E}$ the controller guarantees that the steady-state value of error vector E is zero, which follows from the fact that the controller solves the controller implementation problem. This is in sharp contrast to standard LOS guidance schemes.

IV. Example

In this section we apply the methodology developed in Sec. III to the design and implementation of an integrated guidance and control system for a fixed wing unmanned air vehicle named Bluebird. Bluebird is operated at the Unmanned Air Vehicle Laboratory of the U.S. Naval Postgraduate School. It has a 12.5-ft wingspan and a 35-lb payload capability and is equipped with a full avionics suite, including inertial measurement unit, GPS, and air data sensors.

A. Bluebird Model

Let $\{W\}$ denote the wind axis. It is usually attached to aircraft's center of gravity and is defined using the right-hand rule, with the x axis pointing in the direction of the apparent wind. For example, in the absence of wind the aircraft inertial velocity resolved in $\{W\}$ has the following form: $[\|V\| \;\; 0 \;\; 0]'$. Now let ${}^B_W\mathcal{R}$ denote the transformation from $\{W\}$ to $\{B\}$. Notice, ${}^B_W\mathcal{R}$ can be computed using the angle of attack α and the sideslip angle β, where $\beta = \sin^{-1}(v/\|V\|)$ and $\alpha = \sin^{-1}(w/\|V\|)$. Now, using the notation in Sec. II, the Bluebird dynamics have the following form:

$$\mathcal{G} = \left\{\begin{aligned}\frac{\mathrm{d}}{\mathrm{d}t}V &= \mathcal{F}_V(V,\Omega,\Lambda) + \mathcal{I}_V(V,\Omega)\mathcal{H}(V,\Omega,U)\\ \frac{\mathrm{d}}{\mathrm{d}t}\Omega &= \mathcal{F}_\Omega(V,\Omega,\Lambda) + \mathcal{I}_\Omega(V,\Omega)\mathcal{H}(V,\Omega,U)\\ \frac{\mathrm{d}}{\mathrm{d}t}P &= {}^I_B\mathcal{R}V\\ \frac{\mathrm{d}}{\mathrm{d}t}\Lambda &= \mathcal{Q}\Omega\end{aligned}\right. \qquad (15)$$

Following the development in Sec. II, the set of trimming trajectories $\mathcal{E}$ for Bluebird is defined as follows:

$$\mathcal{E} := \left\{\begin{bmatrix} P_C \\ \Lambda_C \end{bmatrix} : \begin{aligned} &\frac{\mathrm{d}}{\mathrm{d}t}P_C = {}^I_C\mathcal{R}V_C\\ &\frac{\mathrm{d}}{\mathrm{d}t}\Lambda_C = \mathcal{Q}_C\Omega_C\\ &\mathcal{F}_V(V_C,\Omega_C,\Lambda_C)\\ &\quad + \mathcal{I}_V(V_C,\Omega_C)\mathcal{H}(V_C,\Omega_C,U_c) = 0\\ &\mathcal{F}_\Omega(V_C,\Omega_C,\Lambda_C)\\ &\quad + \mathcal{I}_\Omega(V_C,\Omega_C)\mathcal{H}(V_C,\Omega_C,U_c) = 0\end{aligned}\right\} \qquad (16)$$

where P_C and Λ_C can be computed using the scheduling vector $q = [v_c \;\; \gamma_c \;\; \dot{\psi}_c]'$. Now, given $[v_c \;\; \gamma_c \;\; \dot{\psi}_c]'$ and $\beta_c = 0$ we can solve for V_C, Ω_C, U_c, and Λ_C from

$$\begin{aligned}&\mathcal{F}_V(V_C,\Omega_C,\Lambda_C) + \mathcal{I}_V(V_C,\Omega_C)\mathcal{H}(V_C,\Omega_C,U_c) = 0\\ &\mathcal{F}_\Omega(V_C,\Omega_C,\Lambda_C) \;+\; \mathcal{I}_\Omega(V_C,\Omega_C)\mathcal{H}(V_C,\Omega_C,U_c) = 0\\ &\mathcal{Q}_C^{-1}\Omega_C - \dot{\Lambda}_C = 0, \qquad \|V_C\| - v_c = 0\\ &\beta_c - \sin^{-1}(v_c/V_t) = 0, \qquad \gamma_c - [0 \quad 1 \quad 0]\arg\left({}^W_B\mathcal{R}\,{}^B_I\mathcal{R}\right) = 0\end{aligned} \qquad (17)$$

where the arg function extracts the angles X from the rotation matrix $\mathcal{R}(X)$: $X = \arg(\mathcal{R}(X))$ [for example, for straight line flight the last expression in Eqs. (17) reduces to $\gamma_c = \theta_c - \alpha_c$]. Equations (17) consist of 12 equations in 12 unknowns, because the trimming value of the heading angle ψ is arbitrary and can be solved using analytical

or numerical methods. For an example of an interesting analytic solution see Refs. 9 and 16.

Using the solution to Eqs. (17) the linear model for Bluebird represented by Eqs. (10) was obtained along a straight line trajectory characterized by the velocity v_c of 73 fps, γ_c of zero, and wings level ($\dot{\psi}_c = 0$, a typical cruise condition for Bluebird). This model was used to design a linear trajectory tracking controller for the vehicle.

The linear model of the Bluebird in cruise is typical for a fixed wing aircraft, i.e., it naturally decouples into lateral and longitudinal dynamics. The longitudinal dynamics are characterized by a short-period mode with a natural frequency of 0.5 rad/s, a damping ratio of 0.7, and a lightly damped, stable phugoid mode. Lateral dynamics include a lightly damped Dutch roll mode with a damping ratio of 0.03, a roll mode, and an unstable spiral mode. Bluebird utilizes standard elevators, rudder, and differential ailerons for control and a single gas engine driven propeller in the nose for thrust. To ensure appropriate Dutch roll response and rudder behavior in trim we have designed a yaw damper for Bluebird, which washes out rudder in steady state. As a result, the control input vector U available for the trajectory tracking controller consisted of ailerons, elevator, and thrust.

B. Design Requirements and Linear Controller Design

In a calm air mass, tracking inertially fixed trajectories presents no danger to the aircraft because the inertial velocity of the aircraft along the trajectory equals aircraft's velocity with respect to air mass. However, in a changing air mass, attempting to maintain an inertially referenced velocity can lead to the airspeed exceeding the safety limits. Therefore, it is natural to require that the commanded velocity along the inertial trajectory be relative to the air mass, i.e., indicated airspeed. Additional design requirements for the linear trajectory tracking controller included the following: 1) Zero steady-state error: achieve zero steady-state tracking errors of all trajectories in $\mathcal{E}$; achieve zero steady-state tracking of indicated airspeed while on any trajectory in $\mathcal{E}$ in the presence of a constant disturbance. 2) Bandwidth requirements: the command-loop bandwidth for each command channel should be no greater than 1 rad/s and no less than $\frac{1}{10}$ rad/s; the control-loop bandwidth should not exceed 12 rad/s for the elevator, aileron, and rudder loops, and 5 rad/s for the throttle loop. These numbers represent 50% of the corresponding actuator bandwidths and shall ensure that the actuators are not driven beyond their linear operating range. 3) Closed loop damping and stability margins: the dominant closed-loop eigenvalues should have a damping ratio of at least 0.5. Simultaneous gain and phase margins of 6 dB and 45 deg in each control loop must be achieved.

The methodology selected for linear control system design was $\mathcal{H}_\infty$ synthesis.[20] This method rests on a firm theoretical basis and leads naturally to an interpretation of control design specifications in the frequency domain. Furthermore, it provides clear guidelines for the design of controllers so as to achieve robust performance in the presence of plant uncertainty. The basic steps in the controller-design procedure, including the development of the synthesis model, were done using the approach described in Ref. 21. This approach provides an intuitive and straightforward way for converting the design requirements into the weights for the $\mathcal{H}_\infty$ synthesis model. Consider Fig. 4. Here $\mathcal{C}_l$ is the controller to be designed, and $\mathcal{G}_l$ is the linear model of Bluebird.

In Fig. 4 the vector of exogenous inputs w represents input commands. The vector y_1 represents lateral and vertical displacement states of the linear model as well as vehicle's velocity. The regulated output z includes the outputs of the weighting matrices W_1 and W_2. These matrices had the following form:

$$W_1 = \begin{bmatrix} \frac{c_1}{s}\frac{\omega^2}{s^2+\omega^2} & 0 & 0 \\ 0 & \frac{c_2}{s} & 0 \\ 0 & 0 & \frac{c_3}{s} \end{bmatrix}, \qquad W_2 = \begin{bmatrix} c_4 & 0 & 0 \\ 0 & c_5 & 0 \\ 0 & 0 & c_6 \end{bmatrix}$$

where the constants $c_i, i = 1, 6$, were used as the design knobs adjusted to meet the closed-loop tracking, damping, control, and command loop bandwidth requirements. Notice that the structure of W_1 ensures steady-state tracking of constant commands in all three channels and rejection of sinusoidal disturbances at a frequency of ω in the velocity channel as per design requirements. A nominal value of ω was selected and the resulting values of W_1 and W_2 were used to obtain a linear trajectory tracking controller:

$$\mathcal{C}_l := \begin{cases} \delta E = [\delta v \quad \delta y \quad \delta z]' - [\delta v_c \quad \delta y_c \quad \delta z_c]' \\ \dfrac{\mathrm{d}}{\mathrm{d}t}\delta X_{c1} = \mathcal{A}_{c1}\delta X_{c1} + \mathcal{B}_{c1}\delta X_{c2} \\ \dfrac{\mathrm{d}}{\mathrm{d}t}\delta X_{c2} = \delta E \\ \delta U = \mathcal{C}_{c1}\delta X_{c1} + \mathcal{D}_{c1}[\delta V_E' \quad \delta\Omega_E' \quad \delta\Lambda_E']' \\ \quad + \mathcal{D}_{c2}\delta X_{c2} + \mathcal{D}_{c3}\delta E \end{cases}$$

where the $\mathcal{H}_\infty$ state feedback gain is $\mathcal{K} = [\mathcal{C}_{c1} \ \mathcal{D}_{c1} \ \mathcal{D}_{c2} \ \mathcal{D}_{c3}]$ and the matrix $\mathcal{A}_{c1}$ includes the $s/(s^2+\omega^2)$ dynamics. The feedback system consisting of the plant $\mathcal{G}_l$ and the controller $\mathcal{C}_l$ was found to meet all of the design specifications given earlier in this section.

Tracking any trajectory in $\mathcal{E}$ that represents a helix at a constant inertial velocity in a constant wind results in sinusoidal variations of the vehicle's airspeed. The average frequency of the oscillations is equal to the commanded turn rate $\dot{\psi}_C$. This suggests that $\dot{\psi}_C$ can be used as a scheduling variable to ensure disturbance rejection in the velocity channel at that frequency. Furthermore, because the control surface effectiveness is proportional to the dynamic pressure $\bar{q} = 0.5\rho\|V\|^2$, the controller $\mathcal{C}_l$ was gain scheduled on $\bar{q}$ and the commanded turn rate $\dot{\psi}_c$:

$$\mathcal{C}_l(\bar{q}, \dot{\psi}_C) := \begin{cases} \delta E = [\delta v \quad \delta y \quad \delta z]' - [\delta v_c \quad \delta y_c \quad \delta z_c]' \\ \dfrac{\mathrm{d}}{\mathrm{d}t}\delta X_{c1} = \mathcal{A}_{c1}(\dot{\psi}_c)\delta X_{c1} + \mathcal{B}_{c1}\delta X_{c2} \\ \dfrac{\mathrm{d}}{\mathrm{d}t}\delta X_{c2} = \delta E \\ \delta U = \dfrac{\bar{q}_0}{\bar{q}}\{\mathcal{C}_{c1}(\dot{\psi}_c)\delta X_{c1} + \mathcal{D}_{c1}[\delta V' \quad \delta\Omega' \quad \delta\Lambda_E']' \\ \quad + \mathcal{D}_{c2}\delta X_{c2} + \mathcal{D}_{c3}\delta E\} \end{cases}$$

where $\bar{q}_0$ represents the nominal value of $\bar{q}$.

C. Implementation and Simulation Results

Using the formulas provided in Sec. III the family of linear gain scheduled controllers $\mathcal{C}_l(\bar{q}, \dot{\psi}_c)$ was implemented on the nonlinear plant $\mathcal{G}$ as follows:

$$\mathcal{C} := \begin{cases} [0 \quad y \quad z]' = {}^{A}_{I}\mathcal{R}(P - P_C(s_0)) \\ E = [v - v_c \quad y \quad z] \\ \dot{X}_{c1} = \mathcal{A}_{c1}(\dot{\psi}_c)X_{c1} + \mathcal{B}_{c2}E \\ \dot{X}_{c2} = \dfrac{\bar{q}_0}{\bar{q}}\left\{\mathcal{C}_{c1}(\dot{\psi}_c)X_{c1} + \mathcal{D}_{c1}\left[\dfrac{\mathrm{d}}{\mathrm{d}t}V' \quad \dfrac{\mathrm{d}}{\mathrm{d}t}\Omega' \quad \Omega - \mathcal{Q}^{-1}(\Lambda)\dfrac{\mathrm{d}}{\mathrm{d}t}\Lambda_C\right]' + \mathcal{D}_{c3}\dfrac{\mathrm{d}}{\mathrm{d}t}E + \mathcal{D}_{c2}E\right\} \\ U = X_{c2} \end{cases}$$

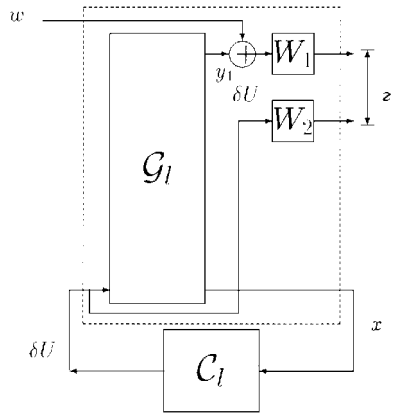

Fig. 4 Synthesis and analysis model.

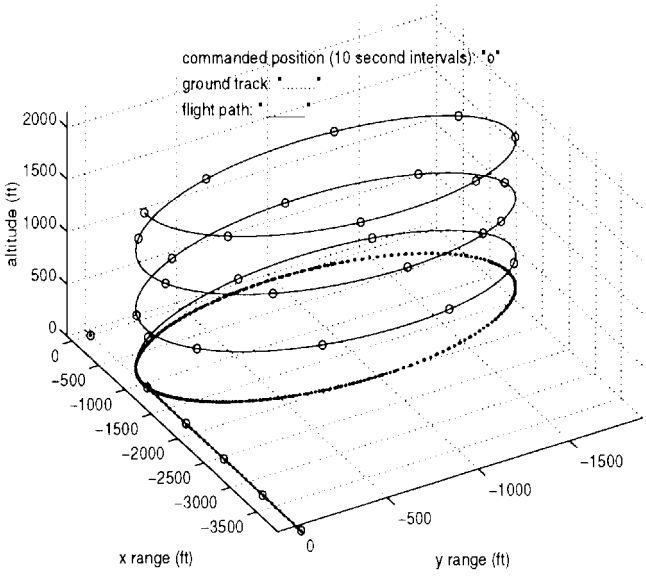

Fig. 5 Helix trajectory.

We emphasize that the implementation equations for the controller $\mathcal{C}$ do not require the computation of Ω_C, U_c, and V_C. Moreover, because $(\mathrm{d}/\mathrm{d}t)\Lambda_C = [0\ 0\ \dot{\psi}_c]'$, the controller must only be provided with $\dot{\psi}_c$ and P_C when steering the aircraft along the trajectory. These are the critical advantages of the proposed methodology. The acceleration term $(\mathrm{d}/\mathrm{d}t)V$ can be computed using onboard sensors without resorting to differentiation. Therefore, the only term that could not be computed directly was $(\mathrm{d}/\mathrm{d}t)\Omega$. In this case the differentiation operator $\mathrm{d}/\mathrm{d}t$ was replaced by a causal operator with the transfer function $s/(\tau s + 1)$ (Ref. 11).

The trajectory tracking controller just developed was tested using a number of trajectories. One such trajectory consisted of a straight line transitioning into a helix (shown in Fig. 5). This trajectory is characterized by a typical Bluebird cruise velocity of 73 fps. Initially, the trajectory is aligned with the inertial x axis. After proceeding along the x axis for 3000 ft, the trajectory turns into a helix with a radius of 1000 ft and climb angle of 5 deg. Consider Fig. 6, which shows the time history of the position error, bank and pitch angles, and indicated airspeed along the trajectory. Clearly, the controller drives Bluebird along this trajectory with zero steady-state position errors while maintaining 73 fps indicated airspeed.

Next, the simulation was repeated, this time with changing air mass. A constant wind velocity of 20 fps in the positive y direction was introduced at the start of the run. The results are summarized in Fig. 7. During the first segment of the trajectory the wind is seen as a constant disturbance by the controller. The aircraft "crabs" into the prevailing wind as expected. This is confirmed by the zero bank angle. The lateral and vertical position errors are driven to zero. When the vehicle turns onto the helix approximately 40 s into the simulation, the wind, which is constant in the inertial frame, is seen as a sinusoidal disturbance in the body frame. Using the

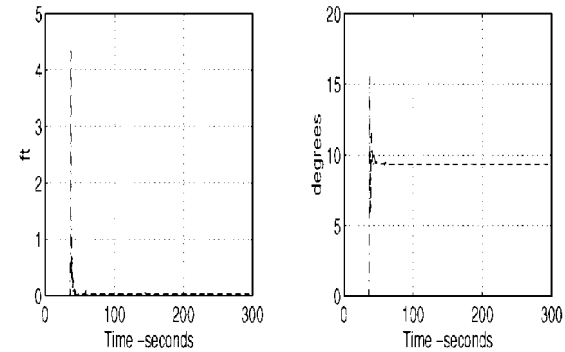

Magnitude of position error **Bank angle**

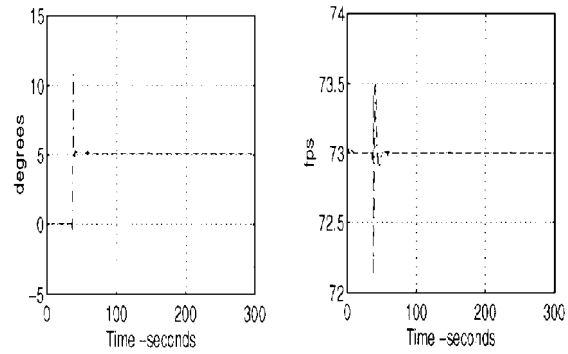

Pitch angle **Indicated airspeed**

Fig. 6 Position error, pitch and bank angles, and velocity.

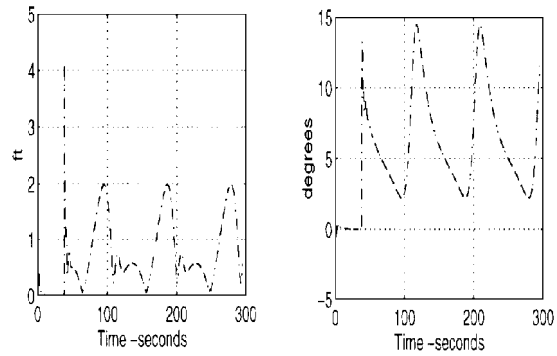

Magnitude of position error **Bank angle**

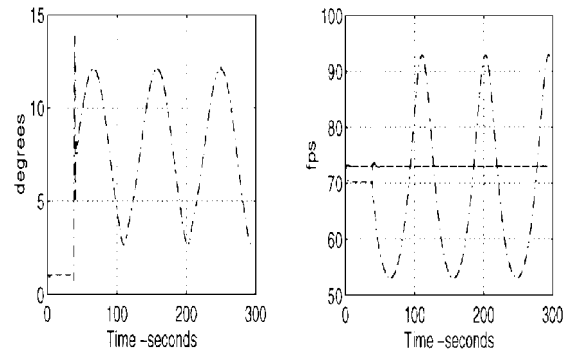

Pitch angle **IAS (- - -) and groundspeed (–·–)**

Fig. 7 Position error, pitch and bank angles, and velocity in the presence of wind.

commanded indicated airspeed and a measured value of the wind, the controller determines the commanded instantaneous turn rate $\dot{\psi}_C$ to reject disturbances in indicated airspeed. This can be seen on the bottom right plot of Fig. 7, which shows that an indicated airspeed of 73 fps is maintained while the inertial velocity oscillates between 53 and 73 fps. Furthermore, while on the helix the controller allows for small position errors resulting from the fact that in the presence of the wind the inertial trajectory is no longer a trimming trajectory. This is confirmed by a time-varying bank angle plot in the upper right corner of Fig. 7.

V. Conclusions

A new method was introduced for designing and implementing integrated guidance and control systems for autonomous vehicles. The starting point is a family of linear controllers with integral action designed for linearizations of the nonlinear equations of motion described in an appropriate state space. Based on this family, the method produces a gain scheduled controller that preserves the input–output properties of the original linear closed-loop systems as well as the closed-loop eigenvalues. The key feature of the method is the ability to automatically reconfigure the control inputs of the vehicle to provide for proper control action as the body tracks an inertial trajectory in free space while maintaining constant airspeed. The method is simple to apply and leads to a nonlinear controller with a structure similar to that of the original linear controllers.

Appendix: Error Dynamics and Their Linearization

A. Derivation of Eq. (9)

Note, we only need to derive the expression for $(\mathrm{d}/\mathrm{d}t)\Lambda_E$. Recall that $\Lambda_E = \mathcal{Q}^{-1}(\Lambda - \Lambda_C)$. Therefore,

$$\frac{\mathrm{d}}{\mathrm{d}t}\Lambda_E = \mathcal{Q}^{-1}\left(\frac{\mathrm{d}}{\mathrm{d}t}\Lambda - \frac{\mathrm{d}}{\mathrm{d}t}\Lambda_C\right) + \frac{\mathrm{d}}{\mathrm{d}t}\mathcal{Q}^{-1}(\Lambda - \Lambda_C)$$

and because $(\mathrm{d}/\mathrm{d}t)\Lambda = \mathcal{Q}\Omega$ and $(\mathrm{d}/\mathrm{d}t)\Lambda_C = \mathcal{Q}_C\Omega_C$, we obtain

$$\frac{\mathrm{d}}{\mathrm{d}t}\Lambda_E = \Omega - \mathcal{Q}^{-1}\mathcal{Q}_C\Omega_C + \frac{\mathrm{d}}{\mathrm{d}t}\mathcal{Q}^{-1}(\Lambda - \Lambda_C) \tag{A1}$$

B. Derivation of Eq. (10)

To obtain Eq. (10) we need the following identity.

Identity 1: Let ${}^I_B\mathcal{R}$ be the rotation matrix from $\{B\}$ to $\{I\}$, and let $\mathcal{Q}$ satisfy $(\mathrm{d}/\mathrm{d}t)(\Lambda) = \mathcal{Q}\Omega$. Then for any vector X in $\mathcal{R}^3$

$$\frac{\mathrm{d}}{\mathrm{d}\Lambda}\left({}^I_B\mathcal{R}X\right) = -{}^I_B\mathcal{R}\mathcal{S}(X)\mathcal{Q}^{-1} \tag{A2}$$

and

$$\frac{\mathrm{d}}{\mathrm{d}\Lambda}\left({}^B_I\mathcal{R}X\right) = \mathcal{S}\left({}^B_I\mathcal{R}X\right)\mathcal{Q}^{-1} \tag{A3}$$

Proof: First, we observe that[15]

$$\frac{\mathrm{d}}{\mathrm{d}t}\left({}^I_B\mathcal{R}\right) = {}^I_B\mathcal{R}\mathcal{S}(\Omega) \tag{A4}$$

Next, from definition of cross product we get

$$\mathcal{S}(X)Y = -\mathcal{S}(Y)X \tag{A5}$$

for any $X, Y \in \mathcal{R}^3$. Now, using Eqs. (A4), (A5), and the fact that X is a constant vector, we obtain

$$\begin{aligned}\frac{\mathrm{d}}{\mathrm{d}t}\left({}^I_B\mathcal{R}X\right) &= \frac{\mathrm{d}}{\mathrm{d}t}\left({}^I_B\mathcal{R}\right)X + {}^I_B\mathcal{R}\frac{\mathrm{d}}{\mathrm{d}t}X \\ &= {}^I_B\mathcal{R}\mathcal{S}(\Omega)X = -{}^I_B\mathcal{R}\mathcal{S}(X)\Omega\end{aligned} \tag{A6}$$

Next, observe that

$$\frac{\mathrm{d}}{\mathrm{d}t}\left({}^I_B\mathcal{R}X\right) = \frac{\mathrm{d}}{\mathrm{d}\Lambda}\left({}^I_B\mathcal{R}X\right)\frac{\mathrm{d}}{\mathrm{d}t}\Lambda = \frac{\mathrm{d}}{\mathrm{d}\Lambda}\left({}^I_B\mathcal{R}X\right)\mathcal{Q}\Omega \tag{A7}$$

Equation (A2) now follows by comparing Eqs. (A6) and (A7).

To obtain Eq. (A3) note that

$$\frac{\mathrm{d}}{\mathrm{d}t}\left({}^B_I\mathcal{R}\right) = -{}^B_I\mathcal{R}\frac{\mathrm{d}}{\mathrm{d}t}\left({}^I_B\mathcal{R}\right){}^B_I\mathcal{R} = -\mathcal{S}(\Omega){}^B_I\mathcal{R} \tag{A8}$$

Therefore,

$$\frac{\mathrm{d}}{\mathrm{d}t}\left({}^B_I\mathcal{R}X\right) = -\mathcal{S}(\Omega){}^B_I\mathcal{R}X = \mathcal{S}\left({}^B_I\mathcal{R}X\right)\Omega \tag{A9}$$

Moreover, using the chain rule it follows that

$$\frac{\mathrm{d}}{\mathrm{d}t}\left({}^B_I\mathcal{R}X\right) = \frac{\mathrm{d}}{\mathrm{d}\Lambda}\left({}^B_I\mathcal{R}X\right)\frac{\mathrm{d}}{\mathrm{d}t}\Lambda = \frac{\mathrm{d}}{\mathrm{d}\Lambda}\left({}^B_I\mathcal{R}X\right)\mathcal{Q}\Omega \tag{A10}$$

Equation (A3) follows readily from Eqs. (A9) and (A10).

Finally, let $\Lambda = 0$, then

$${}^I_B\mathcal{R} = {}^B_I\mathcal{R} = \mathcal{Q} = I$$

Using Eqs. (A2) and (A3), we get

$$\frac{\mathrm{d}}{\mathrm{d}\Lambda}\left({}^I_B\mathcal{R}X\right)\Big|_{\Lambda=0} = \frac{\mathrm{d}}{\mathrm{d}\Lambda}\left({}^B_I\mathcal{R}X\right)\Big|_{\Lambda=0} = \mathcal{S}(X) \tag{A11}$$

□

Now, observe that we only need to derive the expressions for $(\mathrm{d}/\mathrm{d}t)\delta P_E$ and $(\mathrm{d}/\mathrm{d}t)\delta\Lambda_E$. Let

$$\mathcal{M} = \begin{bmatrix} 1 - y\kappa & 0 & 0 \\ z\tau & 1 & 0 \\ y\tau & 0 & 1 \end{bmatrix}^{-1} = \begin{bmatrix} (1 - y\kappa)^{-1} & 0 & 0 \\ -z\tau(1 - y\kappa)^{-1} & 1 & 0 \\ -y\tau(1 - y\kappa)^{-1} & 0 & 1 \end{bmatrix}$$

Then,

$$\frac{\mathrm{d}}{\mathrm{d}t}P_E = \mathcal{M}^A_B\mathcal{R}V$$

Furthermore,

$$\begin{aligned}\frac{\mathrm{d}}{\mathrm{d}t}\delta P_E &= \frac{\partial}{\partial P_E}\left[\mathcal{M}^A_B\mathcal{R}V\right]\Big|_c\delta P_E + \frac{\partial}{\partial\Lambda_E}\left[\mathcal{M}^A_B\mathcal{R}V\right]\Big|_c\delta\Lambda_E \\ &\quad + \frac{\partial}{\partial V}\left[\mathcal{M}^A_B\mathcal{R}V\right]\Big|_c\delta V\end{aligned} \tag{A12}$$

Using simple algebra we obtain

$$\frac{\partial}{\partial P_E}\left[\mathcal{M}^A_B\mathcal{R}V\right]\Big|_c = \left({}^A_C\mathcal{R}V_C\right)_x\begin{bmatrix} 0 & \kappa & 0 \\ 0 & 0 & -\tau \\ 0 & -\tau & 0 \end{bmatrix} \tag{A13}$$

where the subscript c implies that the preceding gradient is being evaluated along the trimming trajectory. From the definition of Λ_E, it follows that

$$\frac{\partial\Lambda}{\partial\Lambda_E} = \mathcal{Q} \tag{A14}$$

Next, using Eq. (A14) and Identity 1, we get

$$\begin{aligned}\frac{\partial}{\partial\Lambda_E}\left[\mathcal{M}^A_B\mathcal{R}V\right]\Big|_c &= \left(\mathcal{M}\frac{\partial}{\partial\Lambda_E}\left[{}^A_B\mathcal{R}V\right]\right)\Big|_c \\ &= \left(\frac{\partial}{\partial\Lambda_E}\left[{}^A_I\mathcal{R}{}^I_B\mathcal{R}V\right]\right)\Big|_c = -\left({}^A_I\mathcal{R}\frac{\partial}{\partial\Lambda}\left[{}^I_B\mathcal{R}V\right]\frac{\partial\Lambda}{\partial\Lambda_E}\right)\Big|_c \\ &= -\left({}^A_I\mathcal{R}{}^I_B\mathcal{R}\mathcal{S}(V)\mathcal{Q}^{-1}\mathcal{Q}\right)\Big|_c = -{}^A_C\mathcal{R}\mathcal{S}(V_C)\end{aligned} \tag{A15}$$

and

$$\frac{\partial}{\partial V}\left[\mathcal{M}^A_B\mathcal{R}V\right]\Big|_c = {}^A_C\mathcal{R} \tag{A16}$$

By combining Eqs. (A13–A16) we obtain the desired expression for $(\mathrm{d}/\mathrm{d}t)\delta P_E$.

By observing that along the trajectories $P_C \in \mathcal{E}$ $(\mathrm{d}/\mathrm{d}t)\mathcal{Q}^{-1} = 0$ and using simple algebra we obtain

$$\frac{\mathrm{d}}{\mathrm{d}t}\delta\Lambda_E = \delta\Omega_E - \frac{\partial}{\partial\Lambda}\left(\mathcal{Q}^{-1}\frac{\mathrm{d}}{\mathrm{d}t}\Lambda_C\right)\frac{\partial\Lambda}{\partial\Lambda_E}\Big|_c\delta\Lambda_E \tag{A17}$$

Because $\dot{\Lambda}_C = [0\ \ 0\ \ \dot{\psi}_c]$ and from the definition of $\mathcal{Q}$ (Ref. 17), it follows that

$$\mathcal{Q}^{-1}\frac{\mathrm{d}}{\mathrm{d}t}\Lambda_C = {}^B_I\mathcal{R}\frac{\mathrm{d}}{\mathrm{d}t}\Lambda_C \tag{A18}$$

Finally, using Identity 1 and Eqs. (A14) and (A18) we obtain:

$$\begin{aligned}\frac{\partial}{\partial\Lambda}\left(\mathcal{Q}^{-1}\frac{\mathrm{d}}{\mathrm{d}t}\Lambda_C\right)\frac{\partial\Lambda}{\partial\Lambda_E}\Big|_c &= \frac{\partial}{\partial\Lambda}\left({}^B_I\mathcal{R}\frac{\mathrm{d}}{\mathrm{d}t}\Lambda_C\right)\mathcal{Q}\Big|_c \\ &= \mathcal{S}\left({}^B_I\mathcal{R}\frac{\mathrm{d}}{\mathrm{d}t}\Lambda_C\right)\mathcal{Q}^{-1}\mathcal{Q}\Big|_c = \mathcal{S}(\Omega_C)\end{aligned} \tag{A19}$$

The desired expression for $(\mathrm{d}/\mathrm{d}t)\delta\Lambda_E$ now follows from expressions (A17) and (A19).

C. Computation of $P_C(s_0)$ and s_0

Let P denote the position of the body. Then the projection $P_C(s_0)$ of P onto the helix $P_C \in \mathcal{E}$ is a solution to the following optimization problem:

$$\begin{aligned} &\min \|P - P_C(s_0)\| \\ &\text{subject to} \\ &P_C(s) \in P_C \end{aligned} \tag{A20}$$

This problem can be reduced to an unconstrained optimization problem over s_0. Let $P_C(s_0) = [x \;\; y \;\; z]'$, then $x = r\cos[(\dot{\psi}_C/v_c)s_0]$, $y = r\cos[(\dot{\psi}_C/v_c)s_0]$, and $z = \dot{h}_c s_0/v_c$, where r and $\dot{h}_c$ denote the radius and the climb rate of the helix, respectively (see Sec. II). Suppose $P = [x_1 \;\; y_1 \;\; z_1]'$. The optimization problem (A20) can be rewritten as follows:

$$\begin{aligned} \min_{s_0} &\left[x_1 - r\cos\left(\frac{\dot{\psi}_C}{v_c}s_0\right)\right]^2 + \left[y_1 - r\cos\left(\frac{\dot{\psi}_C}{v_c}s_0\right)\right]^2 \\ &+ \left(z - \frac{\dot{h}_c s_0}{v_c}\right)^2 \end{aligned} \tag{A21}$$

This problem, in general, does not have an analytical solution and, therefore, must be solved numerically. In practice, an iterative solution based on Newton's method can be used. For the case of a circle ($\dot{h}_c = 0$), however, the analytical solution is simply the point that lies on the intersection of the circle with the line connecting the circle's origin with the vehicle. Let

$$R(\pm) := \left[\pm\sqrt{r^2\frac{x_1^2}{x_1^2 + y_1^2}} \quad \pm\sqrt{r^2\frac{y_1^2}{x_1^2 + y_1^2}} \quad z_1\right]'$$

The solution to Eq. (A20) for the case of a circle is $P_C(s_0) = \operatorname{argmin}_{\pm}\|P - R(\pm)\|$, and if $P_C(s_0) = [x \;\; y \;\; z]$, then $s_0 = (v_c/\dot{\psi}_C)\tan^{-1}(y/x)$.

Acknowledgment

This work was supported in part by Naval Air Systems Command under the Maritime Avionics Subsystems Technology Program. I. Kaminer received partial support from a NATO Fellowship during his stay at Instituto Superior Técnico in Lisbon, Portugal. The work of A. Pascoal and C. Silvestre was supported by Junta Nacional de Investigação Cientifica e Tecnologica under Contract PMCT/C/TIT/702/90 and by two NATO scholarships during their stay at the U.S. Naval Postgraduate School. Reference 3 is available from NASA_News@mercury.hq.nasa.gov.

References

[1]Pascoal, A. M., "The AUV MARIUS: Mission Scenarios, Vehicle Design, Construction and Testing," *Proceedings 2nd Workshop on Mobile Robots for Subsea Environments*, Monterey, CA, Univ. of Southwestern Louisiana, 1994.

[2]Costello, D., Kaminer, I., Carder, K., and Howard, R., "The Use of Unmanned Vehicle Systems for Coastal Ocean Surveys: Scenarios for Joint Underwater and Air Vehicle Missions," *Proceedings 1995 Workshop on Intelligent Control of Autonomous Vehicles* (Lisbon, Portugal), 1995, pp. 61–72.

[3]Douglas, I., and Koehler, K., "Low-Cost Aircraft Navigation System to Aid Global Climate Change Studies," NASA News Release 96-99, May 1996.

[4]Slattery, R. A., and Zhao, Y., "En-Route Descent Trajectory Synthesis for Air Traffic Control Automation," *Proceedings 1995 American Control Conference* (Seattle, WA), 1995, pp. 3430–3434.

[5]Papoulias, F., "Stability Considerations of Guidance and Control Laws for Autonomous Underwater Vehicles in the Horizontal Plane," *Proceedings 7th International Symposium on Unmanned Untethered Vehicle Technology* (Durham, NH), 1991, pp. 140–158.

[6]Healey, A., and Lienard, D., "Multivariable Sliding Mode Control for Autonomous Diving and Steering of Unmanned Underwater Vehicles," *IEEE Journal of Oceanic Engineering*, Vol. 18, No. 3, 1993, pp. 327–339.

[7]Lin, C., *Modern Navigation, Guidance, and Control Processing*, Prentice–Hall, Englewood Cliffs, NJ, 1991.

[8]Fryxell, D., Oliveira, P., Pascoal, A., Silvestre, C., and Kaminer, I., "Navigation, Guidance and Control of AUVs: An Application to the MARIUS Vehicle," *Control Engineering Practice*, Vol. 4, No. 3, 1996, pp. 401–409.

[9]Silvestre, C., Pascoal, A. M., Fryxell, D., and Kaminer, I., "Design and Implementation of a Trajectory Tracking Controller for an Autonomous Underwater Vehicle," *Proceedings 1995 American Control Conference* (Seattle, WA), 1995, pp. 2975–2979.

[10]Kaminer, I., Hallberg, E., Pascoal, A., and Silvestre, C., "On the Design and Implementation of a Trajectory Tracking Controller for a Fixed Wing Unmanned Air Vehicle," *Proceedings 1995 American Control Conference* (Seattle, WA), 1995, pp. 2970–2974.

[11]Kaminer, I., Pascoal, A., Khargonekar, P., and Coleman, E., "A Velocity Algorithm for the Implementation of Gain-Scheduled Controllers," *Automatica*, Vol. 3, No. 8, 1995, pp. 1185–1191.

[12]Samson, C., "Path Following and Time-Varying Feedback Stabilization of a Wheeled Mobile Robot," *Proceedings International Conference ICARCV'92*, Singapore, 1992 (RO-13.1).

[13]Walsh, G., Tilbury, D., Sastry, S., Murray, R., and Laumond, J. P., "Stabilization of Trajectories for Systems with Nonholonomic Constraints," *IEEE Transactions on Automatic Control*, Vol. 39, No 1, 1994, pp. 216–222.

[14]Godhavn, J. M., "Nonlinear Tracking of Underactuated Surface Vessels," *Proceedings 36th IEEE Conference on Decision and Control* (Kobe, Japan), 1996, pp. 975–981.

[15]Craig, J. J., *Robotics*, Addison–Wesley, Reading, MA, 1989.

[16]Elgersma, M., "Control of Nonlinear Systems Using Partial Dynamic Inversion," Ph.D. Thesis, Dept. of Electrical Engineering, Univ. of Minnesota, Minneapolis, MN, 1988.

[17]Roskam, J., *Airplane Flight Dynamics and Automatic Flight Controls,* Roskam Aviation and Engineering Corp., Ottawa, KS, 1979.

[18]Baxandall, P., and Liebeck, H., *Vector Calculus*, Clarendon, Oxford, England, UK, 1986.

[19]Rugh, W. J., "Analytical Framework for Gain Scheduling," *IEEE Control Systems Magazine*, Vol. 11, No. 1, 1991, pp. 74–84.

[20]Doyle, J., Glover, K., Khargonekar, P., and Francis, B., "State Space Solutions to Standard $\mathcal{H}_2$ and $\mathcal{H}_\infty$ Control Problems," *IEEE Transactions on Automatic Control*, Vol. AC-34, No. 8, 1989, pp. 831–847.

[21]Kaminer, I., "Motion Control of Rigid Bodies Using $\mathcal{H}_\infty$ Synthesis and Related Theory," Ph.D. Thesis, EECS Dept., Univ. of Michigan, Ann Arbor, MI, Dec. 1992.